Superconducting Magnet for a Helium-Driven Disk MHD Generator

T. Okamura,* S. Kabashima,† and S. Shioda‡
Tokyo Institute of Technology, Yokohama, Japan

Design studies on superconducting magnets coupled with a full-scale (1000 MWth) closed-cycle disk MHD generator are described. Special attention is given to a new supporting structure that can sustain a large electromagnetic force induced between the windings in Helmholtz-type magnets; and the feasibility of this structure is examined. It is shown that the magnet is expected to become considerably compact.

Nomenclature

A = cross-sectional area of channel
$\boldsymbol{B}$ = magnetic field vector
C_f = friction coefficient of wall
C_p = heat capacity under constant pressure
D = pebble diameter
$\boldsymbol{E}$ = electric field vector
E_r = Hall electric field
e = electron charge
G = gas mass flow rate per unit area of pebble bed
g_c = dimensional constant
g_i = statistical weight of ground state of ith atom
g_i^+ = statistical weight of ground state of ith ion
H = height of pebble bed
h = Plank's constant
$\boldsymbol{J}$ = current density vector
J_r = Hall current density
k = Boltzmann's constant
m_e = electron mass
m_j = mass of jth particle
N_{st} = Stanton number
n_e = concentration of electron
n_{He} = concentration of helium atom
n_{iO} = total concentration of ith atom and ion
n_i^+ = concentration of ith ion
P = gas pressure
Qr = radiation loss
S = circumference of channel
T_e = electron temperature
T_g = gas temperature
T_w = wall temperature
T_{g0w} = adiabatic wall temperature
$\boldsymbol{u}$ = velocity vector
z = axial coordinate
β = Hall parameter
β_{eff} = effective Hall parameter
ϵ = void fraction of bed
ϵ_i = ionization potential of ith atom
μ = viscosity of gas
ν_{ej} = collision frequency between electron and jth particle
$\nu_{e\text{-}He}$ = collision between electron and helium atom
ρ = mass density of gas
σ = electrical conductivity
σ_{eff} = effective electrical conductivity
$< >$ = spatial average

Received July 2, 1986; revision received Nov. 10, 1986.

*Graduate Student, Department of Energy Sciences.
†Associate Professor, Department of Energy Sciences.
‡Professor, Department of Energy Sciences.

Introduction

TO improve the efficiency of electric powerplants fired by fossil fuels, the closed combined MHD-magnet cycle is proposed.[1] In an application of a disk MHD generator to this system, one of the major concerns is to know whether or not a full-scale superconducting magnet coupled with the generator can be constructed at an acceptable level of the present technology. As a first step toward this problem, design studies on the possible configurations of the magnet are carried out in the present work.

The design of a superconducting magnet requires specifying the generator size and magnetic field strength. However, this is complicated because the generator size depends on the magnetic field distribution in the MHD channel. Hence, sizes of both the generator and the winding must be calculated simultaneously.

In this work, an optimized configuration of a Helmholtz-type magnet coupled with a disk MHD generator is considered, in which two circular windings face each other with a space between to accommodate the generator. In this case, special care has to be taken to support the separated windings against the large electromagnetic attractive body force induced between them, while keeping heat leakage as low as possible. A new supporting structure is proposed to meet these requirements. On the other hand, in order to eliminate the supporting structure problem, studies on a configuration in which a single-winding magnet is coupled with the MHD generator are also carried out. The present design approach is relatively conservative, putting emphasis on a reliable and economical magnet.

Full-Scale Disk-Type MHD Generator

A typical configuration of a disk MHD generator is shown in Fig. 1. Both sides of the disk are attached to hot ducts through which the working gas (potassium-seeded helium) enters the nozzle and then flows along the radial direction of the disk. As a working gas, helium has the following advantages over argon: 1) due to its high velocity and resultant high-power density, both the MHD channel and the superconducting magnet can be compact; 2) it has a high ionization potential and therefore the nonequilibrium plasma has a wider stable region of electron temperature against ionization instability[2]; 3) its high thermal conductivity permits the use of compact recuperative heat exchangers in the powerplant.

The thermal input to the present full-scale supersonic MHD generator is assumed to be 1000 MW and the enthalpy extraction and isentropic efficiency are specified to be 35 and 75%, respectively. The Mach number for the flow at the outlet of the MHD channel is close to unity, leading to better diffuser efficiency. The basic design parameters for the present disk MHD channel are listed in Table 1.

In the present work, the procedures are as follows. First, the parameters for an MHD generator are determined for a cer-

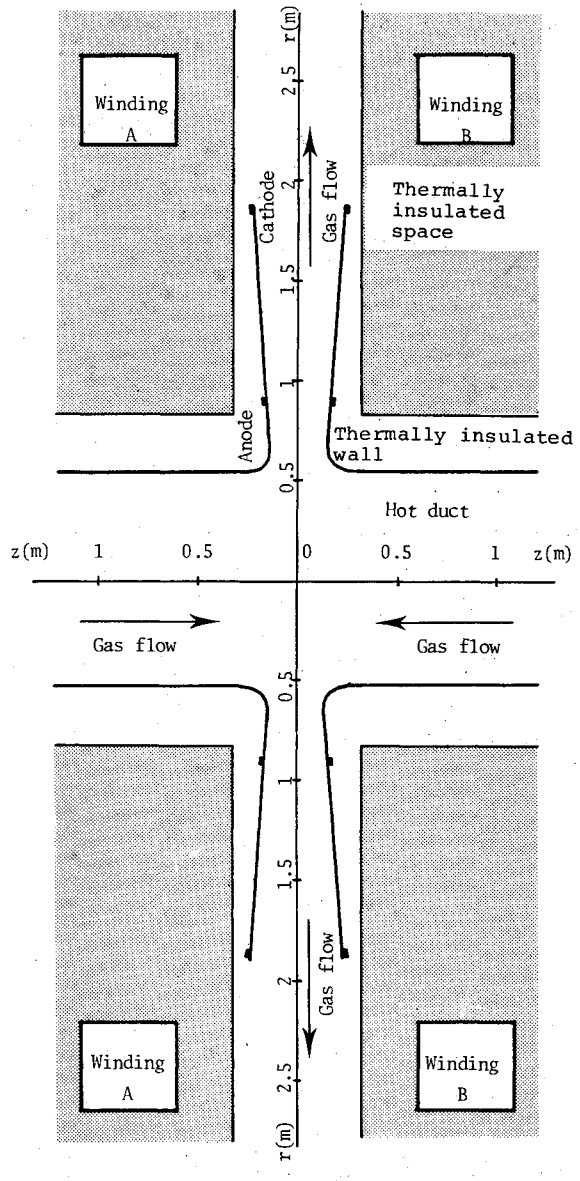

Fig. 1 Typical configuration of a disk MHD generator with 1000 MW thermal input.

Table 1 Basic conditions adopted for design of an MHD channel

Thermal input	1000 MW
Working fluid	He + K
Enthalpy extraction	35%
Isentropic efficiency	75%
Seed fraction	1×10^{-5}
Gas temperature	2000 K
Wall temperature	600 K
Electron temperature	6000 K
Outlet Mach number	1.2
Loading factor	0.13

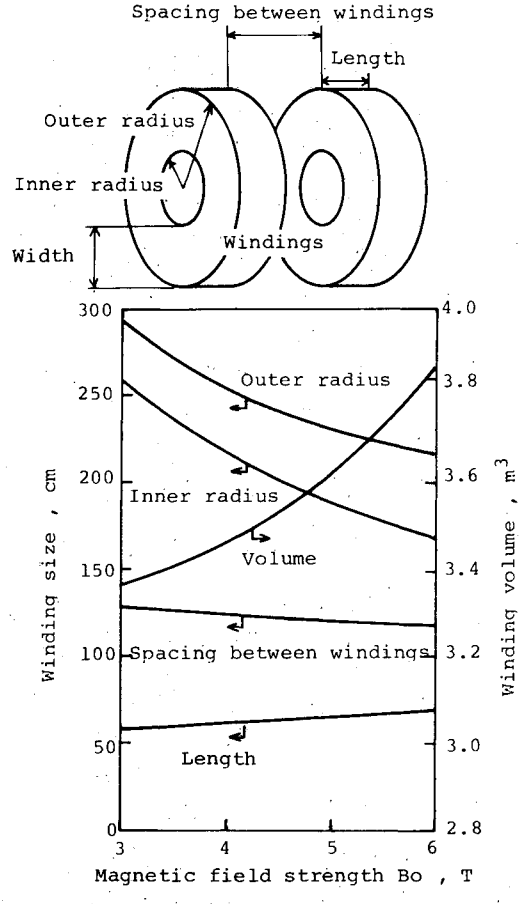

Fig. 2 Size and volume of the winding for various magnetic field strengths at the disk center.

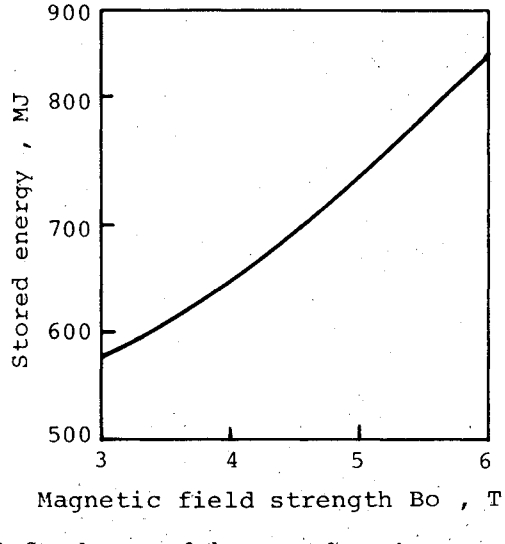

Fig. 3 Stored energy of the magnet for various magnetic field strengths at the disk center.

tain magnetic field strength *Bo* at the center of the disk. Then, several shapes of winding that satisfy this value of *Bo* and provide the necessary space for the generator and thermal insulation are considered. In this study, the shape of the winding cross section is assumed to be rectangular. The magnetic field distribution in the MHD channel is calculated for each winding shape. The minimum volume of the windings is the criterion for selecting the most appropriate winding shape, which will be described in the next section. The performance of the generator under the magnetic field distribution for a given *Bo* is calculated on the basis of one-dimensional MHD equations[2] under the condition of a fully ionized seed. The detailed numerical procedure for the calculation is shown in Appendix A.

The outer radius and length of the winding are selected under the same requirement of minimum winding volume mentioned above. The results for the dimensions and volume of the winding as functions of *Bo* are shown in Fig. 2. It can be seen from this figure that the power density decreases and the MHD channel size (the radii of the anode and cathode and the

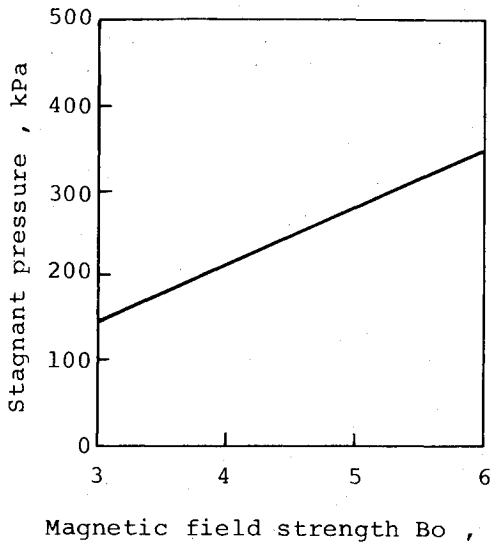

Fig. 4 Stagnant pressure at the MHD channel inlet for various magnetic field strengths at the disk center.

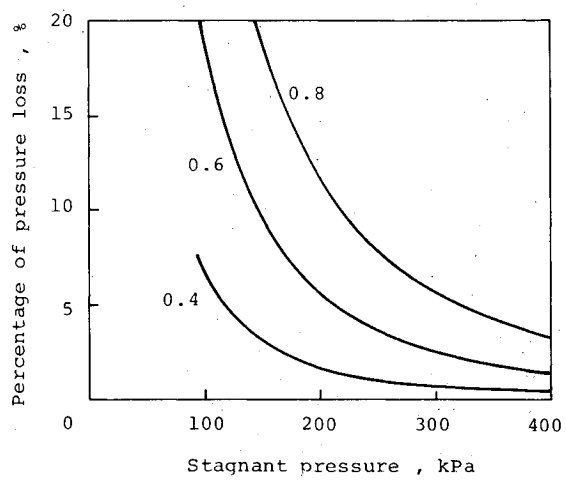

Fig. 5 Percentage of pressure loss in a pebble-bed heat exchanger as a function of the stagnant pressure at the MHD channel inlet (numbers identifying curves indicate helium mass flow rate, kg/m^2·s).

height of the channel) increases as the magnetic field strength *Bo* decreases and that, correspondingly, the inner radius of the windings and the space between the two windings increases. However, both the winding length and width are reduced and thus the winding volume becomes smaller for smaller *Bo*. The stored energy of the magnet tends to decrease with a decrease in *Bo*, as shown in Fig. 3.

The value of *Bo* is chosen based on several considerations. Figure 4 shows the relation between the stagnant pressure at the MHD channel inlet and the magnetic field *Bo* for a condition of 35% enthalpy extraction/75% isentropic efficiency. This relation results because a Hall parameter of about 10 is required for an efficient disk MHD generator with a 75% isentropic efficiency (see Appendix B) for the case of no-swirl flow of helium gas at the inlet of the disk. From Fig. 4, it is observed that the stagnant pressure becomes smaller as the magnetic field decreases.

Furthermore, it is known from model calculations[3] that the rate of pressure loss in helium gas passing through a pebble-bed heat exchanger increases abruptly when the stagnant pressure at the MHD channel inlet is less than about 200 kPa, as shown in Fig. 5. (The detailed numerical procedure is shown in Appendix C.)

These results indicate that a helium pressure of around 200–300 kPa seems to be reasonable as the stagnant pressure at a MHD channel inlet. From these considerations, we select the inlet stagnant pressure of 210 kPa, which corresponds to a magnetic field strength *Bo* of 4.0 T at the center of the disk, as shown in Fig. 4.

Table 2 shows the MHD channel parameters that satisfy the required values and conditions mentioned in Table 1. The values listed in this table indicate that the MHD channel can be made relatively compact, that is, the radii of the hot duct, anode, and cathode become 0.51, 0.87, and 1.83 m, respectively. The height of the MHD channel at the location of the cathode is 0.45 m.

Table 2 Parameters of a typical MHD generator

Anode radius	0.87 m
Cathode radius	1.83 m
MHD channel height at cathode location	0.45 m
Hot duct radius	0.51 m
Magnetic field at disk center	4.0 T
Inlet stagnant pressure	210 kPa
Inlet Mach number	1.81
Radial current	19.7 kA
Hall voltage	17.8 kV
$<Jr>$	0.665 A/cm^2
$<Er>$	185 V/cm
<Power density>	123 MW/m^3
$<\beta_{\text{eff}}>$	13.8
$<\sigma_{\text{eff}}>$	10.2 S/m
Pressure ratio, $\frac{\text{Outlet stagnant pressure}}{\text{Inlet stagnant pressure}}$	$\frac{45}{210} \fallingdotseq \frac{1}{4.7}$
Heat loss in the MHD channel	5.7 MW
Pressure loss in the MHD channel	83 kPa

Full-Scale Helmholtz-Type Magnet

On the basis of current technology some basic conditions are assumed for calculating the characteristics of the magnet. The windings are pool cooled at 4.2 K. The average current density in the windings is fixed at 40 A/mm^2, which is a relatively low and conservative value for complete cryostatic stability. The inner radius and spacing between the windings are kept at fixed values of 2.17 and 1.23 m, respectively, taking into account the MHD channel size; however, various possible outer radii of 2.3–5.0 m and winding lengths of 3.8–0.1 m are also considered. The variations in the winding volume and stored energy in the magnet with the outer radius are shown in Figs. 6 and 7, respectively. It can be seen that these two values are minimized at nearly the same outer radius of about 2.55 m. On the other hand, the attractive body force between the windings shows an increasing trend with an increasing outer radius, as shown in Fig. 8. But the induced force can be sustained easily by a proposed structure, which will be explained in the next section. In other words, the condition of the minimum volume becomes the most important factor in the configuration described here.

The parameters of the magnet whose stored energy is 653 MJ are listed in Table 3; the outer radius, inner radius, and length of the winding are 2.55, 2.17, and 0.61 m, respectively, and the weight is 31 tons. The magnetic field distribution in the winding is shown in Fig. 9. Copper-stabilized Nb_3Sn is partially employed at locations where the magnetic field is larger than 7 T and NbTi is used in the others. The magnetic field limit of NbTi for the case having no strain is higher than 7 T, but considering the strain on the conductor induced by the electromagnetic force (details will be described in the next section), this value is reasonable.

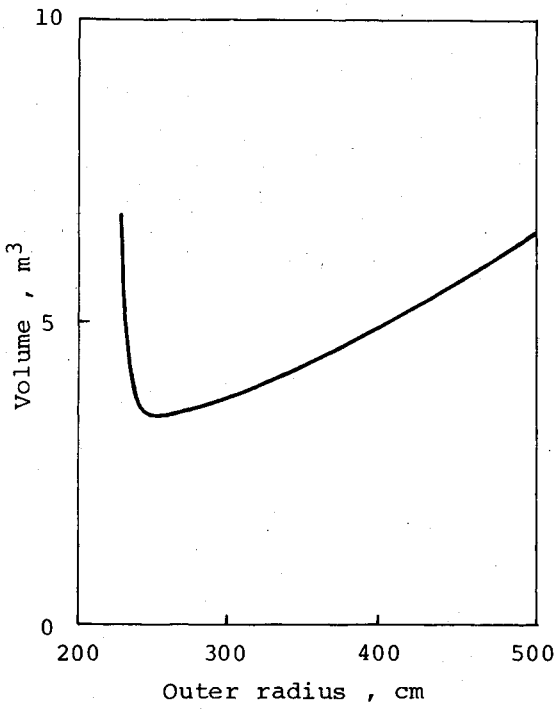

Fig. 6 Variation of volume of the winding with its outer radius.

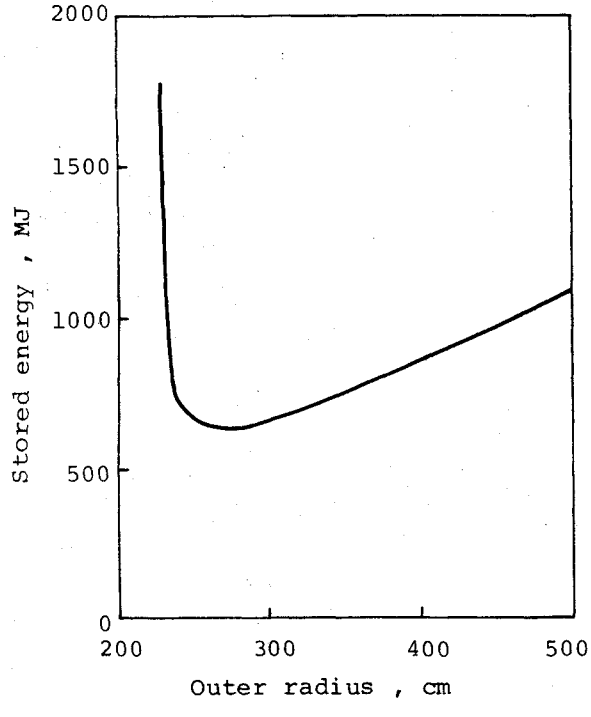

Fig. 7 Variation of stored energy with winding outer radius.

Magnet Assembly

As listed in Table 3, the electromagnetic attractive body force induced between the windings is equivalent to 9884 tons in the case discussed here. Therefore, special care has to be taken to support the separated windings. We propose that the two windings be separated against this force by a helium vessel made of stainless steel, whose overall and assembly layouts, including the MHD generator, are shown in Figs. 10 and 11, respectively. This vessel consists of two winding sections and six rods. Each rod, having the dimensions as

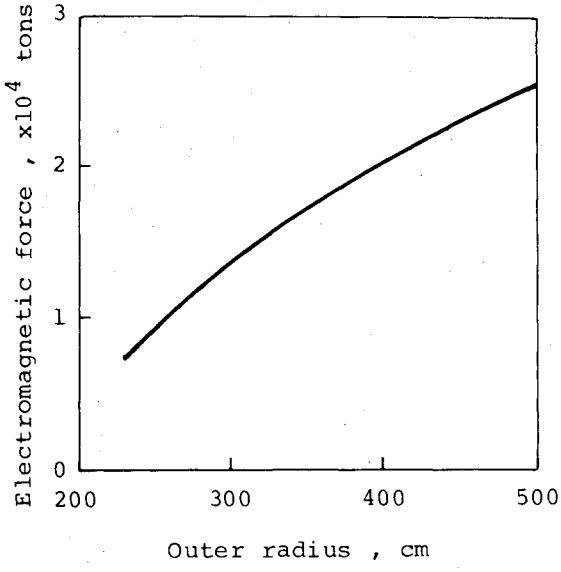

Fig. 8 Variation of attractive body force between the windings with winding outer radius.

Table 3 Parameters of a typical Helmholtz-type superconducting magnet

Winding shape	Circular
Concept on winding	Double pancakes
Concept on cooling	Pool cooling at 4.2 K
Superconductor	NbTi, Nb_3Sn
Rated current	2500 A
Average current density	40 A/mm^2
Winding inner radius	2.17 m
Winding outer radius	2.55 m
Winding length	0.61 m
Spacing between windings	1.23 m
Single-winding weight	31 ton
Magnetic field at disk center	4.0 T
Magnetic field at anode	4.1 T
Magnetic field at cathode	3.6 T
Maximum magnetic field	8.9 T
Electromagnetic attractive body force	9884 ton
Hoop force	1581 ton
Self-inductance	103 H
Mutual inductance	1.9 H
Stored energy	653 MJ

shown in Fig. 12a, penetrates through an insulated space into the diffuser part of the generator channel and is filled with liquid helium. It is noteworthy that the windings are arranged outside of the cathode. The rods serve to support the windings against the attractive body force and the winding sections help them to withstand the circumferential tension (hoop force), since the windings themselves cannot sustain the force.

The generator can be disassembled as follows: the MHD channel section (which should be so arranged as to be easily separated from the diffuser section) can be removed in the z direction and the diffuser (which is divided into six parts) in the radial direction.

The structural analyses of this helium vessel and the windings are carried out using a linear elastic finite-element computer program, "COSMOS6," at the Data Processing Center at Tokyo Institute of Technology. In these calculations, the vessel is assumed to be made of stainless steel 304L and the volume of oxygen-free high conductivity (OFHC) copper and fiber-reinforced plastic (FRP) in the winding is assumed to have a ratio of 78:8; the remaining 14% of the volume is left for the cooling channels. This assumed wind-

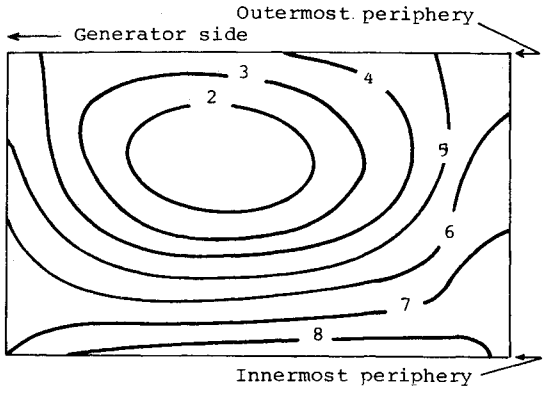

Fig. 9 Magnetic field contour line (interval of 1 T) diagram inside the winding.

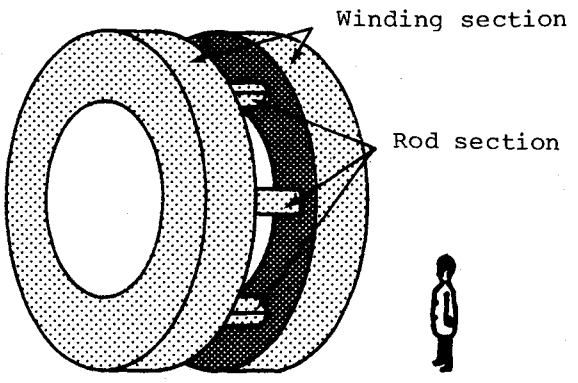

Fig. 10 Outside view of the helium vessel.

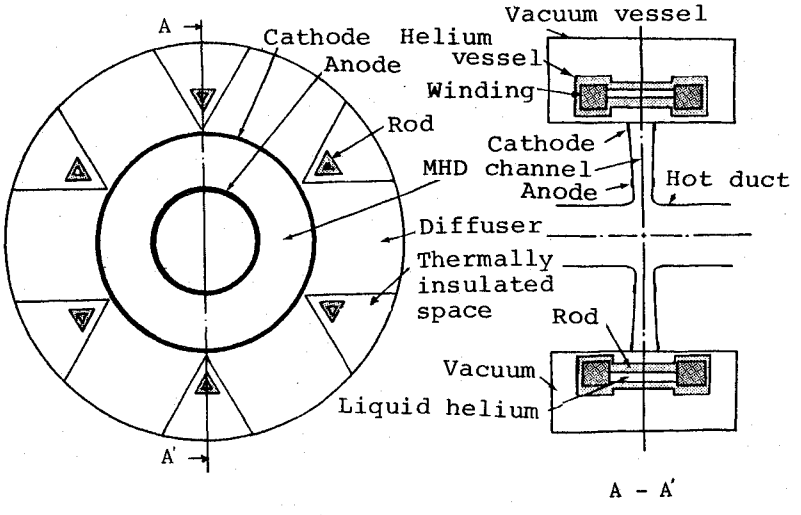

Fig. 11 Layout of the magnet assembly, including the disk MHD generator.

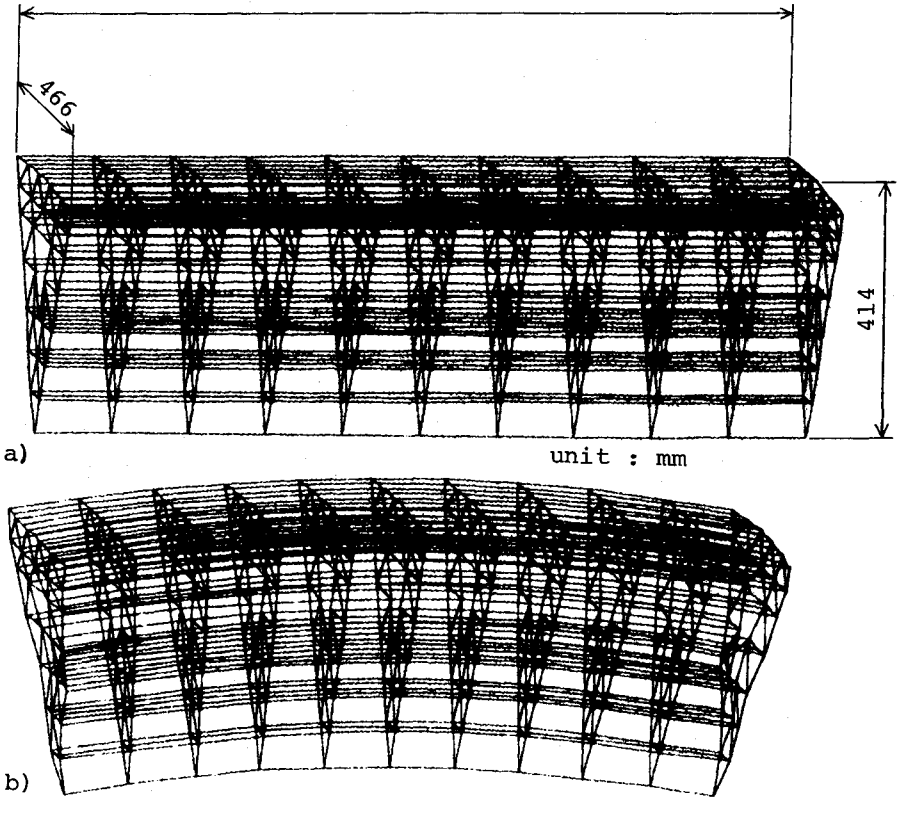

Fig. 12 Connection rod: a) Subdivision of elements to calculate deformation of connection rod (unit in millimeters); b) result of the calculated deformation (deformation displacement enlarged 100 times).

Table 4 Material properties used to calculate deformation of the winding[a]

Stainless stell 304L	Winding
$E=2.020\times10^{11}$	$E\theta=9.427\times10^{10}$
$G=7.924\times10^{10}$	$Er=8.563\times10^{10}$
$N=0.275$	$Ez=2.417\times10^{10}$
	$Gr\theta=3.219\times10^{10}$
OFHC	$G\theta z=3.545\times10^{10}$
$E=1.383\times10^{11}$	$Gzr=3.220\times10^{10}$
$G=5.198\times10^{10}$	$Nr\theta=0.328$
$N=0.33$	$N\theta z=0.251$
	$Nzr=0.242$
FRP	
$E=1.961\times10^{10}$	
$G=6.865\times10^{9}$	
$N=0.3$	

[a] E = modulus of longitudinal elasticity, Pa; G = modulus of transverse elasticity, Pa; N = Poisson's ratio; θ = azimuthal direction; r = radial direction; z = axial direction.

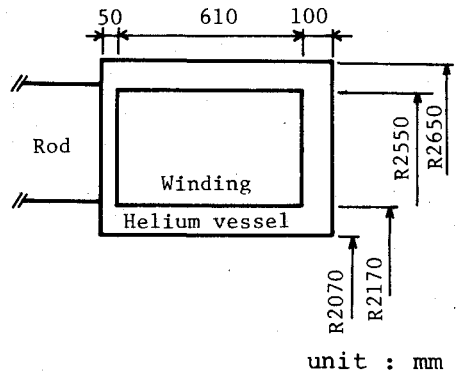

a)

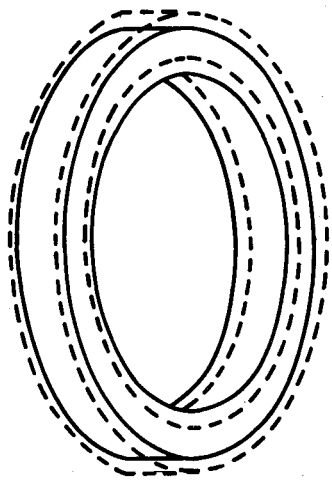

b)

Fig. 13 Winding section: a) cross-sectional view; b) schematic view before (solid line) and after (broken line) deformation (deformation displacement enlarged 100 times).

ing structure with the FRP spacers is believed to be practical, since a similar type of structure is used in the magnet mentioned in Ref. 4, where its conductor's stability is assured. The material properties of these items at 4 K are listed in Table 4. When the magnet is charged, a compressive force of about 1650 tons, which is about 1/75th of the buckling strength, is induced in each rod. As shown in Fig. 12a, the rod is divided into 350 three-dimensional elements; its calculated deformation is shown in Fig. 12b. It is shown that the strain along the central axis is 0.16%, while the

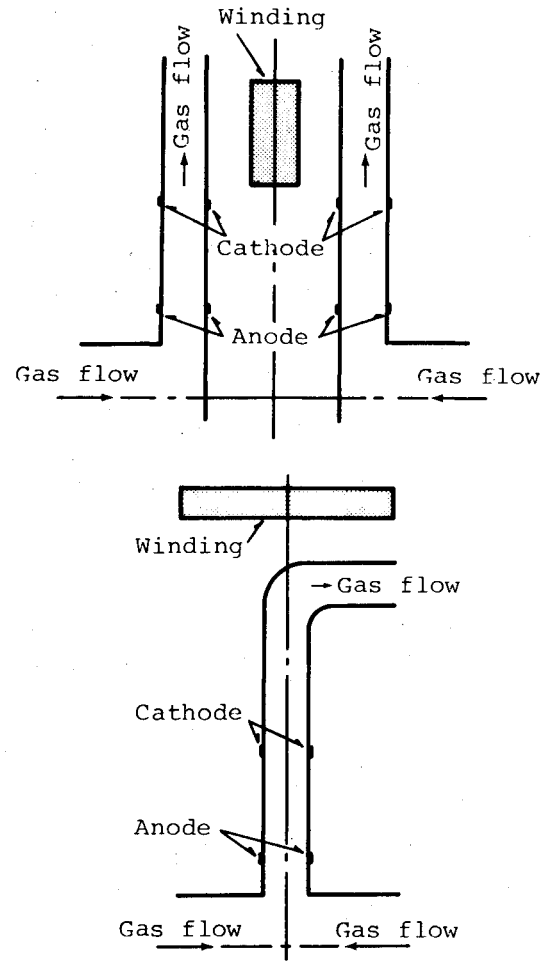

Fig. 14 Typical configuration of a single winding: a) with double disks and b) with a single disk.

strain along the normal to the central axis is only 0.10%. Hence, there is no possibility of breaking.

On the other hand, strain develops in the windings in the tangential direction by hoop force. Generally, this may result in the reduction of the cryostatic stability of a superconductor. Figure 13a shows a cross-sectional view of the present winding section, which is divided into 216 elements. Its outer view before and after deformation is shown in Fig. 13b. It is shown that the maximum strain that develops in the windings along the tangential direction is about 0.98% in the present case. This strain does not have a prominent effect on the stability of the superconductor, as observed from the experiments and analyses mentioned in Refs. 5 and 6.

Thus, the only possible support against the electromagnetic force is the use of a 4.2 K mass. This also assures a significant reduction in heat leakage through thermal conduction.

The helium vessel is enveloped by a vacuum jacket that has a diameter and width of about 5.6 and 3.0 m, respectively. Such dimensions can result in a relatively compact system, including the generator and the magnet.

Single-Winding-Type Magnet

The two circular windings of the Helmholtz-type magnet configuration require special arrangements to keep them separated against the electromagnetic force, as mentioned in the previous section. Therefore, an alternative way to eliminate this key problem is to adopt single-winding magnets.[7] Such a magnet can be coupled with an MHD

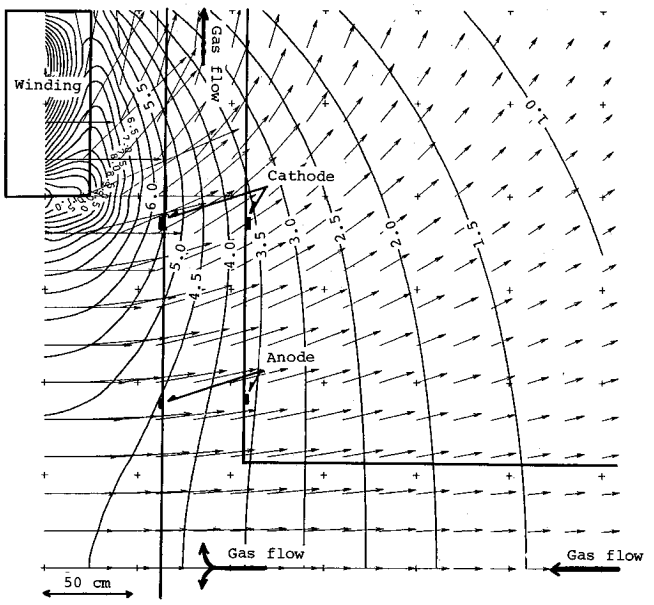

Fig. 15 Magnetic field vector and contour lines (interval of 0.5 T) diagram.

Table 5 Characteristics of a magnet in case of a single winding with double disks

Winding inner radius	2.0 m
Winding outer radius	3.0 m
Winding length	0.45 m
Magnetic field at	
Anode (axial direction)	3.5–4.5 T
Anode (radial direction)	0.7–0.8 T
Cathode (axial direction)	3.0–5.0 T
Cathode (radial direction)	2.1–2.8 T
Hoop force	430 ton
Stored energy	1085 MJ

generators as shown in Fig. 14a, where the winding is placed in between two disk MHD generators.

The design of this single-winding magnet requires the same parameter values (i.e., size of the MHD channel and the thermally insulated space between the winding and MHD channel) as the Helmholtz-type magnet. However, the same magnetic field distribution in the MHD channel is achieved in both cases. Hence, the spatially averaged magnetic field strength in the channel is adjusted to have the same value.

Typical characteristics of this configuration are listed in Table 5. As already discussed, this type of configuration has two major shortcomings that can be expected to disturb the symmetry of helium flow in the disk channel: 1) the magnetic field has its radial components in the MHD channel, as shown in the magnetic field vector diagram of Fig. 15; and 2) there exists a difference of magnetic field of about 1 T between the far and near sides of the channel from the winding, as can be seen in the magnetic field contour diagram of Fig. 15. The radial field components are expected to be reduced by using correction windings in the magnet winding bore,[8] but the difference in the magnetic field strength still remains a problem.

The placement of the generator in the concentric space of the winding (Fig. 14b) is an alternative configuration for eliminating the nonuniformity of the magnetic field. But the stored energy of this magnet becomes about five times larger than that of the Helmholtz-type magnet.

Therefore, it can be concluded from this discussion about single windings that a simple supporting structure against the electromagnetic force can be achieved at the cost of accepting the unfavorable effects of nonuniformity in the magnetic field or enhanced stored energy in the magnet.

Conclusions

The present work indicates the possible construction of full-scale superconducting magnets coupled with disk-type MHD generators. The configuration and assembly layout are clear. Helmholtz-type magnets are more suitable for this type of MHD generator than single-winding ones, because the former may yield the least stored energy and a better uniformity in magnetic field inside the MHD channel.

Although the assumed values of parameters such as the magnetic field strength at the center of the disk and the assumed geometry of the disk channel are not optimized here, the results are not far from reality and, hence, the stored energy of the magnet coupled with helium-driven disk generators is expected to be quite small (less than 1 GJ).

Appendix A: Numerical Procedure for Designing a Disk-Type MHD Generator

Under the assumptions of a two-temperature plasma and a quasi-one-dimensional flow, the steady-state equations for a working gas are written by the equations of plasma as

Saha equilibrium

$$\frac{n_e n_i^+}{n_{i0}-n_i^+}=2\left(\frac{g_i}{g_i^+}\right)\left(\frac{2\pi m_e kT_e}{h^2}\right)^{3/2}\exp\left(\frac{-\epsilon_i}{kT_e}\right) \tag{A1}$$

where $n_e=\sum_i n_i^+$

Energy equation

$$\frac{J^2}{\sigma}=3n_e k(T_e-T_g)\sum_j\left(\frac{m_e}{m_j}\right)\nu_{ej}+Q_r \tag{A2}$$

Ohmic equation

$$\boldsymbol{J}+\left(\frac{\beta}{B}\right)(\boldsymbol{J}\times\boldsymbol{B})=\sigma(\boldsymbol{E}+\boldsymbol{u}\times\boldsymbol{B}) \tag{A3}$$

and together with the following hydrodynamical equations:

Conservation of momentum

$$\frac{\mathrm{d}u_r}{u_r}+\frac{\mathrm{d}P}{\rho u_r^2}-\left(\frac{u_\theta^2}{u_r^2 r}+\frac{J_\theta B}{\rho u_r^2}-C_f\frac{S}{2A}\right)\mathrm{d}r=0 \tag{A4}$$

$$\mathrm{d}u_\theta+\left(\frac{u_\theta}{r}+\frac{J_r B}{\rho u_r}\right)\mathrm{d}r=0 \tag{A5}$$

Conservation of energy

$$\left(\frac{\partial T_g}{\partial P}\right)\frac{\mathrm{d}P}{T_g}+\left[\left(\frac{\partial T_g}{\partial u_r}\right)+\frac{\dot{u}_r}{C_p}\right]\frac{\mathrm{d}u_r}{T_g}+\left[\left(\frac{\partial T_g}{\partial u_\theta}\right)+\frac{u_\theta}{C_p}\right]\frac{\mathrm{d}u_\theta}{T_g}+\left(\frac{\partial T_g}{\partial J_r}\right)\frac{\mathrm{d}J_r}{T_g}=\left[-\frac{J_r E_r}{\rho u_r}-N_{st}C_p(T_{gow}-T_w)\frac{S}{A}\right]\frac{\mathrm{d}r}{C_p T_g} \tag{A6}$$

Continuity:

$$\frac{\mathrm{d}u_r}{u_r}+\frac{\mathrm{d}P}{P}-\frac{\mathrm{d}T_g}{T_g}+\frac{\mathrm{d}z}{z}=-\frac{\mathrm{d}r}{r} \tag{A7}$$

where subscripts r and θ denote the radial and azimuthal component in the cylindrical coordinate system.

To find the geometry of an MHD channel that can maintain a fully ionized seed plasma, we introduce the constraint condition as

$$Te = 6000\text{K (constant throughout the channel)} \qquad \text{(A8)}$$

The following assumptions are made in the numerical calculation: 1) a constant wall temperature along the channel, 2) no voltage drop near the electrodes, 3) no boundary layer (but, friction and heat transfer are included), 4) no impurities in the MHD plasma, 5) no friction and heat losses in the supersonic nozzle, 6) a nozzle wall gradient of 6 deg, and 7) a pressure recovery in the diffuser made by a normal shock. The cross section, heat-transfer coefficient, and friction coefficient used are based on Refs. 9–11.

Appendix B: Relation Between Stagnation Pressure and Magnetic Field Strength at MHD Channel Inlet

The Hall parameter is written as

$$\beta = \frac{eB}{m_e \nu_{ej}} \propto \frac{B}{\nu_{ej}}$$

Because the following relation holds for the present case:

$$\nu_e \fallingdotseq \nu_{e-He} \propto n_{He} \propto P$$

we have

$$\beta \propto B/P$$

which illustrates that the magnetic field strength is proportional to the stagnant pressure.

Appendix C: Pressure Loss in a Pebble-Bed Heat Exchanger

Pressure gradients in a pebble bed are evaluated by[12]

$$\frac{dP}{dz} = 2.4\left(\frac{1-\epsilon}{\epsilon}\right)^{1.1} \frac{1}{\epsilon^2}\left(\frac{GD}{6\mu\epsilon}\right)^{-0.1}\left(\frac{G^2}{g_c D\rho}\right)$$

This question is integrated in the axial direction to obtain the pressure loss of a working gas throughout a bed.

The assumptions made in this calculation are that the temperatures at the top and bottom of a bed are 2100 and 669K respectively, the axial temperature profile in a bed is linear; the void fraction of a bed is 0.4; the pebble diameter is 2 cm; and $H/G = 4.76$ ($m^3 \cdot s/kg$).

Acknowledgments

The authors would like to thank Dr. K. Yoshikawa, Mr. Y. Okuno, and Mr. Y. Sanada for useful discussions.

References

[1]Yoshikawa, K. and Shioda, S., "Closed Cycle MHD Power Generation System Combined with Gas and Steam Turbines," *Proceedings of 2nd Workshop of the Japan-United States Cooperative Program: Basic Studies in MHD Electrical Power Generation,* Montana State University, Bozeman, MN, Vol. 2, 1984, pp. 2.1.1-2.1.35.

[2]Okuno, Y., Kabashima, S., Yamasaki, H., Harada, N., and Shioda, S., "Comparative Studies of the Performance of Closed Cycle Disk MHD Generators Using Argon, Helium and an Argon-Helium Mixture," *Energy Conversion Management,* Vol. 25, March 1985, pp. 345–353.

[3]Yoshikawa, K. and Shioda, S., "Comparative Studies on Ar and He Closed-Cycle MHD Power Plants Combined with Fossil Fuel," *Energy Conversion Management,* Vol. 25, April 1985, pp. 501–506.

[4]Okamura, T., Kabashima, S., Shioda, S., and Sanada, Y., "Superconducting Magnet for a Disc Generator of the FUJI-1 MHD Facility," *Cryogenics,* Vol. 25, Sept. 1985, pp. 483–491.

[5]Ekin, J.W., "Mechanisms for Critical-Current Degradation in NbTi and Nb_3Sn Multifilamentary Wires," *IEEE Transactions on Magnetics,* Vol. MAG-13, Jan. 1977, pp. 127–130.

[6]Ando, T. et al., "10-T, 60-cm Bore Nb_3Sn Test Module Coil Design," *Advances in Cryogenic Engineering,* Vol. 27, 1982, pp. 21–28.

[7]Chubb, D.L. et al., "Assessment of Disk MHD Generator for Base Load Power Plant," *19th Symposium on Engineering Aspects of MHD,* The University of Tennessee Space Institute, 1981, pp. 12.2.1-12.2.14.

[8]Retallick, F.D., "Disk MHD Generator Study," NASA CR-159872.

[9]Mitchener, M. and Kruger, C.H., *Partially Ionized Gases,* Wiley, New York, 1973.

[10]Brederlow, G. and Witte, K.J., "Effective Electrical Conductivity and Related Properties of a Nonequilibrium High Pressure MHD Plasma," *AIAA Journal,* Vol. 12, Jan. 1974, pp. 83–90.

[11]Rosa, R.J., *Magnetohydrodynamic Energy Conversion,* McGraw-Hill, New York, 1968.

[12]Perry, J.H., *Chemical Engineers' Handbook,* 3rd ed. McGraw-Hill, New York, 1950.